



Effect of mixed pinning landscapes produced by 6 MeV oxygen irradiation on the resulting critical current densities J_c in 1.3 μm thick $\text{GdBa}_2\text{Cu}_3\text{O}_{7-\delta}$ coated conductors grown by co-evaporation

N. Haberkorn^{a,b,*}, S. Suárez^{a,b}, P.D. Pérez^a, H. Troiani^{a,b}, P. Granell^c, F. Golmar^{c,d},
Jae-Hun Lee^e, S.H. Moon^e

^a Consejo Nacional de Investigaciones Científicas y Técnicas, Centro Atómico Bariloche, Av. Bustillo 9500, 8400 San Carlos de Bariloche, Argentina.

^b Instituto Balseiro, Universidad Nacional de Cuyo, Av. Bustillo 9500, 8400 San Carlos de Bariloche, Argentina

^c INTI, CMNB, Av. Gral Paz 5445 (B1650KNA), San Martín, Buenos Aires, Argentina

^d Consejo Nacional de Investigaciones Científicas y Técnicas, Escuela de Ciencia y Tecnología, UNSAM, Campus Miguelete, (1650), San Martín, Buenos Aires, Argentina

^e SuNAM Co. Ltd, Ansung, Gyeonggi-Do 430-817, South Korea



ARTICLE INFO

Article history:

Received 13 February 2017

Revised 9 August 2017

Accepted 22 August 2017

Available online 24 August 2017

Keywords:

Coated conductors

Vortex dynamics

Glassy exponents

Irradiation

ABSTRACT

We report the influence of crystalline defects introduced by 6 MeV $^{16}\text{O}^{3+}$ irradiation on the critical current densities J_c and flux creep rates in 1.3 μm thick $\text{GdBa}_2\text{Cu}_3\text{O}_{7-\delta}$ coated conductor produced by co-evaporation. Pristine films with pinning produced mainly by random nanoparticles with diameter close to 50 nm were irradiated with doses between $2 \times 10^{13} \text{ cm}^{-2}$ and $4 \times 10^{14} \text{ cm}^{-2}$. The irradiations were performed with the ion beam perpendicular to the surface of the samples. The J_c and the flux creep rates were analyzed for two magnetic field configurations: magnetic field applied parallel ($\mathbf{H} \parallel c$) and at 45° ($\mathbf{H} \parallel 45^\circ$) to the c -axis. The results show that at temperatures below 40 K the in-field J_c dependences can be significantly improved by irradiation. For doses of $1 \times 10^{14} \text{ cm}^{-2}$ the J_c values at $\mu_0 H = 5 \text{ T}$ are doubled without affecting significantly the J_c at small fields. Analyzing the flux creep rates as function of the temperature in both magnetic field configurations, it can be observed that the irradiation suppresses the peak associated with double-kink relaxation and increases the flux creep rates at intermediate and high temperatures. Under 0.5 T, the flux relaxation for $\mathbf{H} \parallel c$ and $\mathbf{H} \parallel 45^\circ$ in pristine films presents characteristic glassy exponents $\mu = 1.63$ and $\mu = 1.45$, respectively. For samples irradiated with $1 \times 10^{14} \text{ cm}^{-2}$, these values drop to $\mu = 1.45$ and $\mu = 1.24$, respectively

© 2017 Elsevier B.V. All rights reserved.

1. Introduction

During the last years, a great amount of effort has been oriented to improve the superconducting properties of $\text{RBa}_2\text{Cu}_3\text{O}_{7-\delta}$ (RBCO; R: Sm, Dy, Y, Gd) coated superconductors (CCs) [1–4]. One of the strongest aspects expected for applications such as motors and magnets is to be able to maintain high critical current density J_c at high magnetic fields [5,6]. The current carrying capacity is determined by the interaction of vortex matter with crystalline defects [7]. The geometry and density of the pinning centers determine the in-field and angular dependence of J_c [7,8,9]. In addition, the vortex-defect interactions are not accumulative and the vortex pinning produced by the different crystalline defects depends on the temperature and on the magnetic field. While small de-

fects improve pinning mainly below 40 K, large defects (size of a few coherence length ξ) do so throughout the whole temperature range. [10]. For the latter, the pinning can be isotropic (nanoparticles) or correlated (columnar defects). Innovative approaches have been used to design optimal vortex pinning by defect structures [8,11]. Most of them are based on the inclusion of nanometric secondary phases [12,13].

The formation of the desired pinning centers depends sensitively on the film deposition technique and substrate architecture [1,12–14]. Despite the remarkable advance in the synthesis of desirable microstructures obtained at laboratory scale research, pinning landscapes including a high density of strong and weak pinning centers are usually difficult at industrial scale. This limitation in the synthesis of CCs has been recently overcome by including pinning centers by irradiation [15–18]. Depending on the mass and energy of the ions and the properties of the superconducting material, irradiation enables the creation of defects with well-controlled

* Corresponding author.

E-mail address: nhaberk@cab.cnea.gov.ar (N. Haberkorn).

density and topology such as points, clusters, or tracks [19]. The in-field dependence of J_c at temperatures below 40 K has been improved by irradiation with protons in CCS grown by metal organic deposition MOD and co-evaporation [15,16]. Most recently, the feasibility to similarly improve the properties of CCS obtained by MOD in much shorter irradiation times using 3.5 MeV $^{16}\text{O}^{3+}$ has been reported [17].

Here, we show the effects of random point defects and nanoclusters introduced by 6 MeV $^{16}\text{O}^{3+}$ irradiation with doses between $2 \times 10^{13} \text{ cm}^{-2}$ and $4 \times 10^{14} \text{ cm}^{-2}$ on the magnetic field dependence of J_c 1.3 μm thick GBCO thin films grown by co-evaporation. In addition, the vortex dynamics displayed in pristine and irradiated samples is analyzed by performing magnetic relaxation measurements. The microstructure of the pristine tape displays random and irregular shape precipitates with typical size of 50 nm. Unlike ref. [17], the energy of the ions was selected to place the Bragg peak inside the substrate (instead of the superconducting layer). Several attempts of irradiation with 3.5 MeV $^{16}\text{O}^{3+}$ showed that, although the in-field of J_c dependence is smoother than for pristine samples, the irradiation reduces considerably the low field J_c values. In comparison to our previous work [16], in which tapes irradiated with protons reached the optimal doses in tens of minutes, the irradiation with 6 MeV $^{16}\text{O}^{3+}$ demands only a few seconds. While the irradiation significantly improves the in-field dependence of J_c for the $\mathbf{H} \parallel c$ and $\mathbf{H} \parallel 45^\circ$ configurations, its absolute values are merely affected at low fields. From Maley analyses, we calculate the μ glassy exponent for the collective creep regime. For both configurations, the μ values decrease after irradiation, which increases the flux creep rates in comparison to pristine films.

2. Material and methods

The GBCO tape was grown by the co-evaporation technique previously described in refs. [4,20]. The magnetization (\mathbf{M}) measurements were performed by using a superconducting quantum interference device (SQUID) magnetometer with the applied magnetic field (\mathbf{H}) parallel to the c -axis ($\mathbf{H} \parallel c$) and rotated 45° from the c axis ($\mathbf{H} \parallel 45^\circ$). The T_c values used in this work (based on magnetization data) were determined from $M(T)$ at $\mu_0 H = 0.5 \text{ mT}$ applied after zero field cooling. The J_c values were calculated from the magnetization data using the appropriate geometrical factor in the Bean Model. For $\mathbf{H} \parallel c$, $J_c = \frac{20\Delta M}{w(1-w/3l)}$, where ΔM is the difference in magnetization between the top and bottom branches of the hysteresis loop, t is the thickness, and l and w are the length and width of the film ($l > w$), respectively. For $\mathbf{H} \parallel 45^\circ$, both the longitudinal (M_l , parallel to \mathbf{H}) and transversal (M_t , perpendicular to \mathbf{H}) components of \mathbf{M} were measured. Then the irreversible magnetization was calculated as $\Delta M = (\Delta M_l^2 + \Delta M_t^2)^{1/2}$. Using the anisotropic version of the critical state Bean model was obtained $J_c = \frac{20\Delta M}{w(1-\frac{w\cos(45^\circ)}{3l})}$ [21].

The creep rate measurements were recorded for more than 1 h. The initial time was adjusted considering the best correlation factor in the log-log fitting of the $J_c(t)$ dependence. The initial critical state for each creep measurement was generated using $\Delta H \sim 4H^*$, where H^* is the field for full-flux penetration [22]. A good correlation between J_c values obtained by magnetization and by electrical transport in coated conductors at low temperatures has been reported [15].

Irradiation with 6 MeV Oxygen (O-irradiation) produces random point defects and nm-sized anisotropic defects [17,19]. The cumulative amount of displacement damage (displacements per atom, DPA) after each dose (as estimated using the SRIM code [23]), varies from 0.02 up to 0.8 DPA within the sample and for the doses used in the present work. The irradiation was performed at room temperature on pieces with typical area $1.5 \times 1.5 \text{ mm}^2$ using ion beam currents of $\approx 4 \text{ nA}$. In all the cases, the ion beam

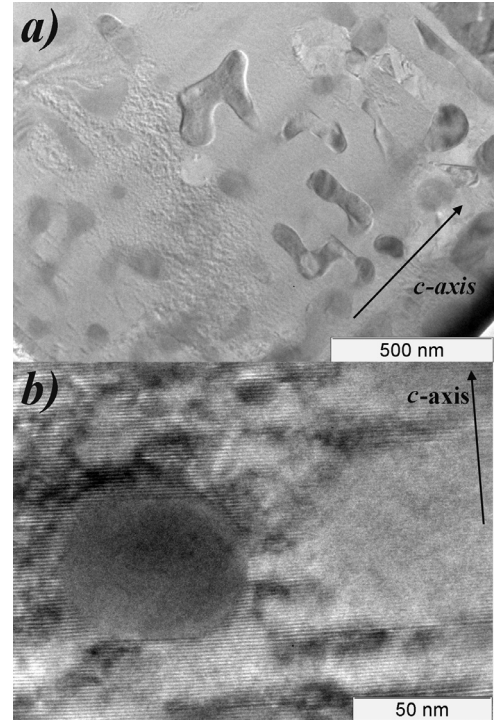


Fig. 1. (a) A TEM image shows typical pinning centers in the GBCO tape. (b) A higher magnification image shows a spherical Gd_2O_3 precipitate with diameter around 50 nm.

was applied perpendicular to the surface of the samples. To guarantee good thermal contact, the samples were fixed to the holder with silver paint. The irradiation spot was 2 mm in diameter, and the homogeneity of the beam was tested impacting in a fluorescent sample (F_2Ca , AlF_3 or LiF), which allowed to take a direct measure of the beam spot dimensions. The irradiations were performed with the ion beam positioned at the center of the sample. Considering the beam spot dimension and the sample geometry (square with size $1.5 \times 1.5 \text{ mm}^2$), the corner of the samples have probably not been homogeneously irradiated. All the samples display similar properties (T_c and $J_c(H, T)$) before irradiation. Wherever used, the notation IRR x indicates a GBCO film without irradiation ($x = 0$); and $x = 2, 4, 6, 10$ and 40 correspond to films irradiated with oxygen dose $2 \times 10^{13} \text{ cm}^{-2}$, $4 \times 10^{13} \text{ cm}^{-2}$, $6 \times 10^{13} \text{ cm}^{-2}$, $1 \times 10^{14} \text{ cm}^{-2}$ and $4 \times 10^{14} \text{ cm}^{-2}$, respectively.

3. Results and discussion

The pinning landscape of pristine films was analyzed from cross-sectional TEM images (Fig. 1a). The microstructure displays sphere-like and irregular precipitates embedded in the GBCO matrix with typical diameter of approximately 50 nm (Fig. 1b). EDS analysis indicates that the precipitates can be associated with Gd_2O_3 . Sphere-like nanoparticles produce isotropic pinning [24]. Irregular precipitates are extended mainly along ab -plane and the c -axis. Nanoparticles aligned at the c -axis are expected to assist correlated pinning usually present in thin films due to defects such as dislocations and twin boundaries [13]. The precipitates are typically spaced between $\sim 100 \text{ nm}$ and 200 nm , which corresponds to an equivalent matching field $< 0.2 \text{ T}$. This is in agreement with high J_c values at low fields and poor in-field dependences [16]. The inclusion of defects by oxygen irradiation in pristine CCS was analyzed in ref. [17]. Similar to proton irradiation, oxygen irradiation creates random point disorder and a large number of finely dispersed small defects ($\phi 5 \text{ nm}$ approximately) [15,17].

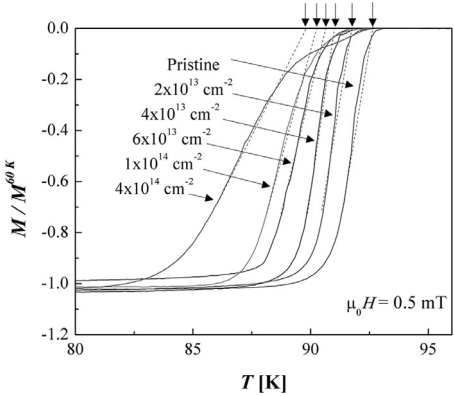


Fig. 2. Temperature dependence of magnetization with $\mu_0 H = 0.5$ mT in the pristine and 6 MeV Oxygen irradiated films. The magnetization value was normalized by its value at 60 K. The magnetic field was applied parallel to the c -axis.

Table 1

Summary of oxygen irradiation dose, superconducting critical temperature (T_c) and glassy exponents for $\mathbf{H} \parallel c$ axis and $\mathbf{H} \parallel 45^\circ$. T_c values were obtained from magnetization in 5 Oe with $\mathbf{H} \parallel c$ -axis after zero field cooling.

Sample	T_c	$\mu \mathbf{H} \parallel c$ -axis	$\mu \mathbf{H} \parallel 45^\circ$
Pristine	92.7 ± 0.2	1.63 ± 0.02	1.45 ± 0.02
$2 \times 10^{13} \text{ cm}^{-2}$	91.8 ± 0.2	1.58 ± 0.02	1.47 ± 0.02
$4 \times 10^{13} \text{ cm}^{-2}$	91.0 ± 0.2	1.59 ± 0.02	—
$6 \times 10^{13} \text{ cm}^{-2}$	90.6 ± 0.2	—	—
$1 \times 10^{14} \text{ cm}^{-2}$	90.2 ± 0.2	1.45 ± 0.02	1.24 ± 0.02
$4 \times 10^{14} \text{ cm}^{-2}$	89.8 ± 0.2	—	—

The T_c in the as-grown film is 92.7 K (see Fig. 2) and is gradually suppressed with the doses. Table 1 shows the T_c values after irradiation. The irradiated samples display a small kink close to zero magnetization, which can be associated with inhomogeneous irradiation at the corners. In addition, irradiated samples display an extended magnetic flux penetration close to T_c . This fact can be associated mainly with weaker vortex pinning due to an increment in the vortex fluctuations close to T_c [25]. The structural disorder produced by the irradiation should increase the penetration length (λ) [26,27]. Also, a slight increment in λ should affect the transition width ΔT_c . Thermal fluctuations broaden the superconducting transition by $\Delta T_c \geq G_i * T_c$ [25], where G_i is the Ginzburg number $G_i = \frac{1}{2} \left[\frac{\gamma T_c}{H_c^2(0) \xi^2(0)} \right]^2$ (with H_c the thermodynamic critical field, γ the mass anisotropy and ξ the coherence length). In optimal doped YBCO ($\lambda = 140$ nm, $T_c = 92$ K, $\gamma = 5$ and $\xi = 1.2$ nm), $G_i \approx 0.018$.

Due to the fact that random disorder and nanoclusters originated by proton and oxygen irradiation produce the most significant changes in J_c at low temperatures [15–17], our study focuses on $J_c(H)$ at temperatures below 40 K. The irradiation for doses larger than IRR2 affects both $J_c(H)$ and the vortex dynamics of the samples. Figs. 3a–c shows a comparison between $J_c(H)$ for IRR0 and IRR10 at 5 K, 27 K and 40 K. The curves display two different regimes. At low fields (regime (I)), J_c is almost constant up to a characteristic crossover field H^* (usually called B^* [28]). Then, it is followed by a power-law regime ($J_c \propto H^{-\alpha}$) at intermediate fields (regime II), observed as a linear dependence on the log-log plot. The main changes produced by the irradiation are manifested at high magnetic fields and can be related to a reduction in the α values. At $\mu_0 H = 5$ T, IRR10 displays J_c values between 1.7 and 2 times larger than IRR0. Figs. 4a–c show the doses dependence of α , $J_c(\mu_0 H = 0)$ and $J_c(\mu_0 H = 3$ T) at 5 K, 27 K and 40 K. The increment in the doses from $2 \times 10^{13} \text{ cm}^{-2}$ to $1 \times 10^{14} \text{ cm}^{-2}$ reduces systematically the α value for the three analyzed tem-

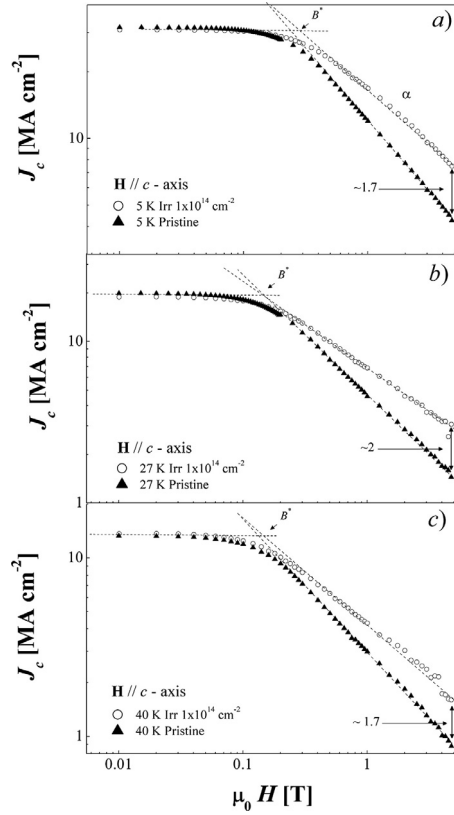


Fig. 3. Magnetic field dependence of the critical current densities for IRR0 and for IRR10 at different temperatures. (a) 5 K; (b) 27 K; and (c) 40 K. All measurements were performed with $\mathbf{H} \parallel c$. The lines between the crossovers are guided by the eye.

peratures without appreciably affecting the J_c values at low fields (Figs 3a and b). For example, at 5 K (relevant for magnets [6]), α is reduced from ≈ 0.64 (IRR0) to $\alpha \approx 0.46$ (IRR10). Although α can be reduced for doses larger than $1 \times 10^{14} \text{ cm}^{-2}$, the damage produced by the irradiation considerably diminishes the J_c values at high magnetic fields (Fig. 4c). The optimal doses for 6 MeV oxygen irradiation ($\approx 1 \times 10^{14} \text{ cm}^{-2}$) is 10 times larger than that described in ref. [17] for 3.5 MeV oxygen irradiation. However, as mentioned above, several attempts of irradiation with 3.5 MeV $^{16}\text{O}^{3+}$ (peak of Bragg within of the GBCO film) showed that, although the in-field J_c dependence is smoother than for pristine samples, the irradiation reduces considerably the low field J_c values.

In order to analyze the influence of the irradiation in the vortex dynamics, magnetic relaxation measurements at $\mu_0 H = 0.5$ T were performed. This field is within the power-law regime discussed above. The giant flux creep rate observed using magnetic relaxation of the persistent currents is well described by the collective vortex creep model based on the elastic properties of the lattice [25]. This model considers that at small fields and with negligible vortex-vortex interaction (single vortex regime SRV), every single-vortex-line is pinned by the collective action of many weak point-like pinning centers (not observed in thin films with strong pinning centers). The vortex-vortex interactions increase as the magnetic field is incremented and the inter-vortex distance is shortened. Hence, the vortices are collectively trapped in bundles. The normalized creep rate $S = -\delta \ln j / \delta \ln t$ is given by $S = \frac{T}{U_0 + \mu T \ln(t/t_0)} = \frac{T}{U_0} \left(\frac{j}{j_c} \right)^\mu$ [Eq. 1], where U_0 is the characteristic energy, $\mu > 0$ is the characteristic glassy exponent and t_0 is a characteristic time. Fig. 5a shows the $S(T)$ dependences for IRR0, IRR2, IRR4 and IRR10. The initial increment of $S(T)$ at low temperatures can be ascribed to an Anderson–Kim-like mechanism with $S \approx T/U$ (with U the pin-

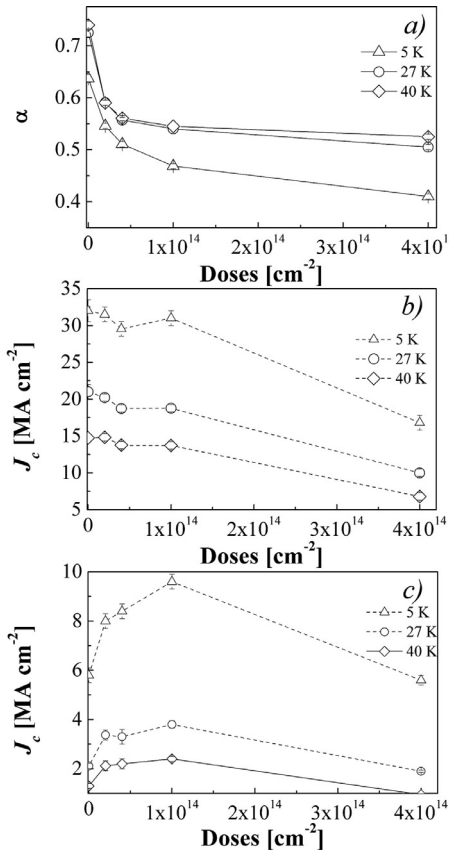


Fig. 4. (a) α versus oxygen doses obtained from $J_c(H) \propto H^{-\alpha}$. In all cases the values are included for 5 K, 27 K and 40 K. (b) Critical current density J_c versus proton doses at $\mu_0 H \rightarrow 0$ for 5 K, 27 K and 40 K. (c) Critical current density J_c versus proton doses at $\mu_0 H = 3$ T for 5 K, 27 K and 40 K.

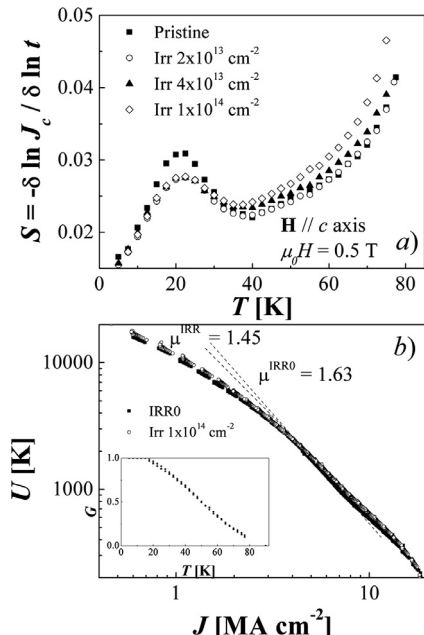


Fig. 5. (a) Temperature dependence of the creep flux rate (S) at $\mu_0 H = 0.5$ T for IRR0 and oxygen irradiated films (IRR2, IRR4 and IRR10). (b) Maley analysis at $\mu_0 H = 0.5$ T for IRR0 and IRR10. The inset shows the $G(T)$ dependences used for the Maley analysis. All measurements were performed with $H \parallel c$ -axis.

ning energy). Non-negligible S values are expected at $T=0$ from quantum creep [25]. At approximately 5 K, all the samples show practically the same $S \approx 0.015$. When the temperature is increased, the $S(T)$ curves present a peak at around 23 K. This is associated with double-kink relaxation due to the presence of correlated pinning. At intermediate temperatures the relaxation displays a minimum with $S(T) \approx \text{constant}$, which is related to glassy relaxation. Finally, at high temperatures, the S values are systematically incremented as consequence of thermal smearing of the pinning potential. The main influence of the irradiation or addition of nanoclusters is the reduction of the double-kink peaks [29]. The expected reduction at the peak is masked by the systematic increment in the S values at the plateau, which can be associated with changes in the μ value that appear in the limit $U_0 < \mu T \ln t/t_0$ and it corresponds to $S \approx \frac{1}{\mu \ln t/t_0}$ [22]. To compare the modifications in the vortex dynamics for GBCO CCs irradiated with protons and oxygen ions, the change in the glassy exponents μ was analyzed by using the extended Maley's method [30]. The effective activation energy $U_{\text{eff}}(J)$ can be experimentally obtained considering the approximation in which the current density decays as $\frac{dJ}{dt} = -(\frac{J_c}{\tau})e^{-\frac{U_{\text{eff}}(J)}{T}}$. The final equation for the pinning energy is $U_{\text{eff}} = -T[\ln|\frac{dJ}{dt}| - C]$ (eq. 2) where $C = \ln(J_c/\tau)$ is nominally a constant factor. For an overall analysis it is necessary to consider the function $G(T)$, which results in $U_{\text{eff}}(J, T=0) \approx U_{\text{eff}}(J, T)/G(T)$ (eq. 3) [31]. Fig. 5b shows the obtained results for IRR0 and IRR10. The inset corresponds to $G(T)$ function. In the limit of $J << J_c$ the μ exponent can be estimated as $\Delta \ln U(J) / \Delta \ln J$ [32]. The μ values obtained at intermediate temperatures are summarized in Table I. The μ value is systematically reduced by the doses, for instance $\mu \approx 1.63$ (IRR0) and $\mu \approx 1.45$ (IRR10).

For a better understanding of the vortex dynamics in the pristine and irradiated films, $J_c(H)$ and magnetic relaxation measurements with $H \parallel 45^\circ$ were performed. Pinning dominated by nanoparticles similar to $J_c(H)$ dependences are expected for $H \parallel c$ and $H \parallel 45^\circ$ [9]. Usually for mix pinning landscapes, synergetic combination of twin boundaries and nanoparticles enhances pinning when $H \parallel c$ [24]. Fig. 6 shows a comparison between $J_c(H)$ for IRR0 and IRR10 at 5 K, 27 K and 40 K. In agreement with the results displayed in Fig. 3 for $H \parallel c$, the irradiation with $H \parallel 45^\circ$ enhances the J_c values by improving the in-field dependence. The J_c values are nearly doubling near $\mu_0 H = 5$ T. Although the $J_c(H)$ dependences can be depicted with a power-law dependence, this behavior is clearly observed for 5 K. At this temperature, α change from ≈ 0.69 (IRR0) to $\alpha \approx 0.47$ (IRR10). For 27 K and 40 K, the $J_c(H)$ dependences display a clear change at intermediate fields which cannot be described by only one pinning mechanism or regime and might be related to relaxation by double-kinks [32]. For an overall understanding of the vortex dynamic in the sample for $H \parallel 45^\circ$ magnetic relaxation measurements at $\mu_0 H = 0.5$ T were carried out. Fig. 7a shows the $S(T)$ dependences for IRR0, IRR2, and IRR10, which can be described by the same mechanism as for $H \parallel c$. An outstanding feature for $S(T)$ with $H \parallel 45^\circ$ is the huge peak associated with relaxation by double-kinks [32,33]. For IRR0 the maximum of the peak is $S \approx 0.04$ and it is extended to temperatures above 40 K. The irradiation reduces considerably this relaxation and it is evidenced in the reduction of the absolute value of S at the maximum of the peak. In addition and in agreement with $H \parallel c$, the irradiation increases the absolute S values at the plateau above 40 K. Fig. 7b shows the Maley analysis for IRR0 and IRR10, where $C=14$ and a $G(T)$ were used (inset Fig. 7b). As well as for $H \parallel c$, the μ value at the collective regime for $H \parallel 45^\circ$ is reduced by the irradiation. The μ values change from $\mu \approx 1.45$ (IRR0) to $\mu \approx 1.24$ (IRR10).

The results show that similar improvement $J_c(H)$ and changes in the vortex dynamics are produced by proton and oxygen irradiation. The main advantage of oxygen is that the optimal doses

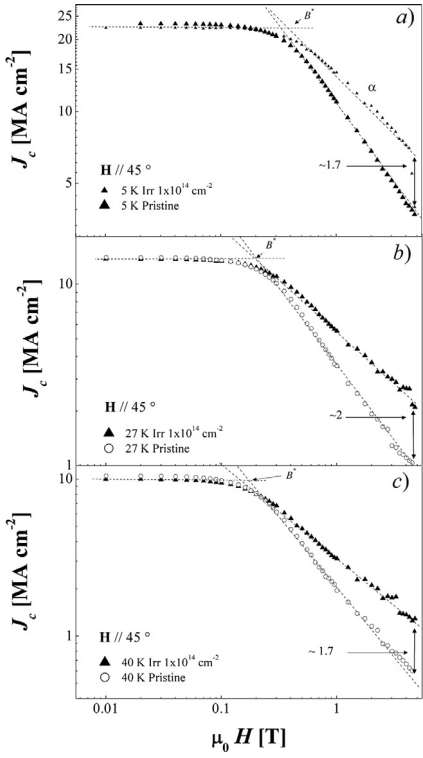


Fig. 6. Magnetic field dependence of the critical current density for IRRO and IRR10 at different temperatures. (a) 5 K; (b) 27 K; and (c) 40 K. All measurements were performed with $\mathbf{H} \parallel 45^\circ$. The lines between the crossovers are guided by the eye.

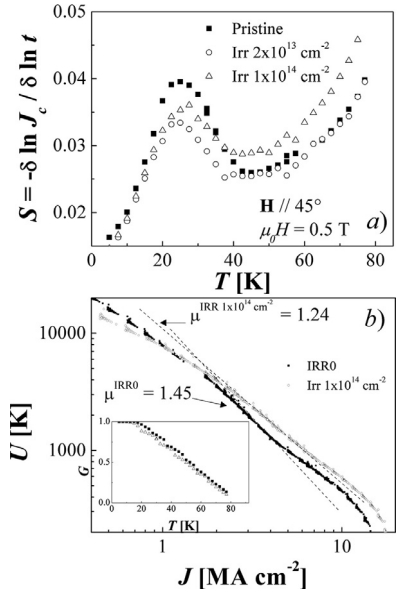


Fig. 7. (a) Temperature dependence of the creep flux rate (S) at $\mu_0 H = 0.5$ T for IRRO, IRR2 and IRR10. (b) Maley analysis at $\mu_0 H = 0.5$ T for IRRO and IRR10. The inset shows $G(T)$ dependences used for the Maley analysis. All measurements were performed with $\mathbf{H} \parallel 45^\circ$.

are reached in shorter time [17]. Our results are focused on 6 MeV $^{16}\text{O}^{3+}$ and on the fact that the peak of Bragg (energy loss) is within the substrate. The optimal dose to improve the in-field dependence of J_c is around $1 \times 10^{14} \text{ cm}^{-2}$. The glassy exponents μ with $\mathbf{H} \parallel c$ is reduced by the irradiation from 1.63 (IRRO) to 1.45 (IRR10). These values are expected for small bundles (3/2–5/2) according to the collective creep model developed for random disorder [25]. It is worth mentioning that pristine 1.3 μm thick YBCO films obtained

by MOD display a plateau with $S \approx 0.02$, which is smaller than that observed in the GdBCO tape studied in this work ($S \approx 0.022$). Assuming $\ln(t/t_0) \approx \text{constant}$, the difference in the S values can be attributed to changes in the vortex bundle size due to different density and morphology of nanoparticles and different density of correlated defects such as TBs. In addition and according to the expectations for pinning by nanoclusters, the irradiation improves the in-field dependence of J_c (H) with $\mathbf{H} \parallel 45^\circ$. At this configuration, the irradiation also suppresses double-kinks and reduces the μ value that dominates the flux creep rates at intermediate temperatures.

The increment in $S(T)$ as a function of irradiation fluency, particularly in the intermediate-temperature plateau and for high temperatures, it is common in CCs grown by MOD and co-evaporation [15–17,34]. As mentioned above, at the plateau $S \approx \frac{1}{\mu \ln(t_0)}$, the vortex dynamics depends on the μ glassy exponent. The vortex dynamics for pristine CCs usually displays $\mu \approx 3/2$ [14,15,34] which successively decreases with doses. No theoretical predictions have been developed for the glassy exponents in mixed pinning landscapes. Recently, the increment in the S values for irradiated samples was correlated with the different type of defects in mixed pinning landscapes [34]. However, the irradiation in CCs modifies both vortex pinning and the intrinsic superconducting properties of the samples. The detrimental of the superconducting properties is usually evidenced as a gradual suppression of T_c [35]. The optimal doses for irradiation results from a balance between the retention of intrinsic superconducting properties and the enhancement of the vortex pinning. As mentioned before, the T_c reduction produced by the irradiation should have a non-negligible contribution in the absolute value of penetration depth λ [27]. In addition, the anisotropy parameter γ is affected by T_c reduction in the oxygen deficient samples [36]. Local changes in the λ value due to structural disorder should affect properties such as the depairing critical current (maximum theoretical J_c in absence of vortex dissipation) and the elasticity of the vortex lattice [25]. The increment in the vortex fluctuations for irradiated samples is in agreement with the huge suppression of J_c at high temperatures [16]. The contribution of the different type of defects and the suppression of the superconducting properties produced by the damage to the vortex mechanisms require further analysis [34,35]. Future studies should be oriented to understand the influence of the irradiation damage (related to T_c suppression) on properties such as λ and γ . These studies should contribute to understand the role of disorder in the balance between the retention of intrinsic superconducting properties and the enhancement of the vortex pinning.

4. Conclusions

In conclusion, we have studied the influence of 6 MeV $^{16}\text{O}^{3+}$ irradiation on the critical current densities J_c and flux creep rates in 1.3 μm thick $\text{GdBa}_2\text{Cu}_3\text{O}_{7-\delta}$ coated conductor produced by co-evaporation. At temperatures below 40 K with $\mathbf{H} \parallel c$ and $\mathbf{H} \parallel 45^\circ$, the critical current density J_c with high magnetic field can be significantly improved by irradiation. For doses of $1 \times 10^{14} \text{ cm}^{-2}$ the J_c values at $\mu_0 H = 5$ T are doubled without affecting significantly the J_c at small fields. Analyzing the flux creep rates as function of the temperature with $\mathbf{H} \parallel c$ and $\mathbf{H} \parallel 45^\circ$, it can be observed that the irradiation suppresses the peak associated with double-kink relaxation and increases the flux creep rates at intermediate and high temperatures. The increment in the flux creep rates at intermediate temperatures can be associated with a reduction in the characteristic glassy exponent μ . While the increment in the flux creep rates at high temperatures may be related with larger vortex fluctuations for irradiated samples. Future studies should be oriented to understand the influence of the irradiation damage (related to T_c suppression) on properties such as λ and γ . An overall under-

standing of the relationship between pinning and the increment in the vortex fluctuations due to disorder is necessary for the optimization of pinning landscapes in CCs.

Acknowledgment

We thank C. Olivares for technical assistance. This work has been partially supported by [Agencia Nacional de Promoción Científica y Tecnológica PICT 2015-2171](#). N. H. is member of the Instituto de Nanociencia y Nanotecnología - CNEA (Argentina).

References

- [1] X. Obradors, T. Puig, S. Ricart, M. Coll, J. Gazquez, A. Palau, X. Granados, Growth, nanostructure and vortex pinning in superconducting $\text{YBa}_2\text{Cu}_3\text{O}_7$ thin films based on trifluoroacetate solutions, *Supercond. Sci. Technol.* 25 (2012) 123001–123032.
- [2] Yuh Shiohara, Takahiro Taneda, Masateru Yoshizumim, Overview of materials and power applications of coated conductors project, *Jpn. J. Appl. Phys.* 51 (2012) 010007–100722.
- [3] M. Heydari Gharacheshmeh, E. Galstyan, A. Xu, J. Kukunuru, R. Katta, Y. Zhang, G. Majkic, X.-F. Li, V. Selvamanickam, Superconducting transition width (ΔT_c) characteristics of 25 mol% Zr-added $(\text{Gd},\text{Y})\text{Ba}_2\text{Cu}_3\text{O}_{7-\delta}$ superconductor tapes with high in-field critical current density at 30 K, *Supercond. Sci. Technol.* 30 (2017) 015016–015022.
- [4] Jae-Hun Lee, Hunju Lee, Jung-Woo Lee, Soon-Mi Choi, Sang-Im Yoo, Seung-Hyun Moon, RCE-DR, a novel process for coated conductor fabrication with high performance, *Supercond. Sci. Technol.* 27 (2014) 044018–044023.
- [5] Carmine Senatore, Matteo Alessandrini, Andrea Lucarelli, Riccardo Tediosi, Davide Ugliesti, Yukikazu Iwasa, Progresses and challenges in the development of high-field solenoidal magnets based on RE123 coated conductors, *Supercond. Sci. Technol.* 27 (2014) 103001–103026.
- [6] Sangwon Yoon, Jaemin Kim, Kyekun Cheon, Hunju Lee, Seungyong Hahn, Seung-Hyun Moon, 26 T 35 mm all- $\text{GdBa}_2\text{Cu}_3\text{O}_{7-x}$ multi-width no-insulation superconducting magnet, *Supercond. Sci. Technol.* 29 (2016) 04LT04 1–6.
- [7] S.R. Folty, L.Civale J.L.Macmanus-Driscoll, Q.X. Jia, B. Maiorov, H. Wang, M. Maley, Materials science challenges for high-temperature superconducting wire, *Nat. Mater.* 6 (2007) 631–642.
- [8] J.L. MacManus-Driscoll, S.R. Folty, Q.X. Jia, H. Wang, A. Serquis, L. Civale, B. Maiorov, M.E. Hawley, M.P. Maley, D.E. Peterson, Strongly enhanced current densities in superconducting coated conductors of $\text{YBa}_2\text{Cu}_3\text{O}_{7-x} + \text{BaZrO}_3$, *Nat. Mat.* 3 (2004) 439–443.
- [9] N. Haberkorn, M. Miura, J. Baca, B. Maiorov, I. Usov, P. Dowden, S.R. Folty, T.G. Holesinger, J.O. Willis, K.R. Marken, T. Izumi, Y. Shiohara, L. Civale, High-temperature change of the creep rate in $\text{YBa}_2\text{Cu}_3\text{O}_7$ films with different pinning landscapes, *Phys. Rev. B* 85 (2012) 174504–174510.
- [10] J. Albrecht, M. Djupmyr, S. Brück, Universal temperature scaling of flux line pinning in high-temperature superconducting thin films, *J. Phys.: Condens. Matter* 19 (2007) Article 216211.
- [11] Kaname Matsumoto, Paolo Mele, Artificial pinning center technology to enhance vortex pinning in YBCO coated conductors, *Supercond. Sci. Technol.* 23 (2010) 014001–014012.
- [12] V. Selvamanickam, M. Heydari Gharacheshmeh, A. Xu, Y. Zhang, E. Galstyan, Critical current density above $15\text{M}\text{Acm}^{-2}$ at 30 K, 3T in 2.2 μm thick heavily-doped $(\text{Gd},\text{Y})\text{Ba}_2\text{Cu}_3\text{O}_x$ superconductor tapes, *Supercond. Sci. Technol.* 28 (2015) 072002–072006.
- [13] M. Miura, B. Maiorov, J.O. Willis, T. Kato, M. Sato, T. Izumi, Y. Shiohara, L. Civale, The effects of density and size of BaMO_3 ($M=\text{Zr, Nb, Sn}$) nanoparticles on the vortex glassy and liquid phase in $(\text{Y,Gd})\text{Ba}_2\text{Cu}_3\text{O}_y$ coated conductors, *Supercond. Sci. Technol.* 26 (2013) 035008–025014.
- [14] N. Haberkorn, Y. Coulter, A.M. Condó, P. Granell, F. Golmar, H.S. Ha, S.H. Moon, Vortex creep and critical current densities J_c in a 2 μm thick $\text{SmBa}_2\text{Cu}_3\text{O}_{7-\delta}$ coated conductor with mixed pinning centers grown by co-evaporation, *Supercond. Sci. Technol.* 29 (2016) 075011–075017.
- [15] Y. Jia, et al., Doubling the critical current density of high temperature superconducting coated conductors through proton irradiation, *Appl. Phys. Lett.* 103 (2013) Article 122601.
- [16] N. Haberkorn, Jeehoon Kim, S. Suárez, Jae-Hun Lee, S.H. Moon, Influence of random point defects introduced by proton irradiation on the flux creep rates and magnetic field dependence of the critical current density J_c of co-evaporated $\text{GdBa}_2\text{Cu}_3\text{O}_{7-\delta}$ coated conductors, *Supercond. Sci. Technol.* 28 (2015) 125007–125012.
- [17] M. Leroux, et al., Rapid doubling of the critical current of $\text{YBa}_2\text{Cu}_3\text{O}_{7-\delta}$ coated conductors for viable high-speed industrial processing, *Appl. Phys. Lett.* 107 (2015) Article 192601.
- [18] I.A. Sadovskyy, et al., Toward superconducting critical current by design, *Adv. Mater.* 28 (2016) 4593–4600.
- [19] Wai-Kwong Kwok, Ulrich Welp, Andreas Glatz, Alexei E. Koshelev, Karenj. Kihlstrom, George W. Crabtree, Vortices in high-performance high-temperature superconductors, *Rep. Prog. Phys.* 79 (2016) 116501–116539.
- [20] J.L. MacManus-Driscoll, M. Bianchetti, A. Kursumovic, G. Kim, W. Jo, H. Wang, J.H. Lee, G.W. Hong, S.H. Moon, Strong pinning in very fast grown reactive co-evaporated $\text{GdBa}_2\text{Cu}_3\text{O}_7$ coated conductors, *APL Materials* 2 (2014) 086103–086110.
- [21] N. Haberkorn, et al., Influence of random point defects introduced by proton irradiation on critical current density and vortex dynamics of $\text{Ba}(\text{Fe}_{0.925}\text{Co}_{0.075})_2\text{As}_2$ single crystals, *Phys. Rev. B* 85 (2012) 014522–014528.
- [22] Y. Yesurun, A.P. Malozemoff, A. Shaulov, Magnetic relaxation in high-temperature superconductors, *Rev. Mod. Phys.* 68 (1996) 911–949.
- [23] J.F. Ziegler, J.P. Biersack, U. Littmark, *The Stopping and Range of Ions in Solids*, Pergamon, New York, 1985.
- [24] M. Miura, B. Maiorov, S.A. Baily, N. Haberkorn, J.O. Willis, K. Marken, T. Izumi, Y. Shiohara, L. Civale, Mixed pinning landscape in nanoparticle-introduced $\text{YGdBa}_2\text{Cu}_3\text{O}_y$ films grown by metal organic deposition, *Phys. Rev. B* 83 (2011) 184519–184526.
- [25] G. Blatter, M.V. Feigelman, V.B. Geshkenbein, A.I. Larkin, V.M. Vinokur, Vortices in high-temperature superconductors, *Rev. Mod. Phys.* 66 (1994) 1125–1388.
- [26] N. Basov, A.V. Puchkov, R.A. Hughes, T. Strach, J. Preston, T. Timusk, D.A. Bonn, R. Liang, W.N. Hardy, Disorder and superconducting-state conductivity of single crystals of $\text{YBa}_2\text{Cu}_3\text{O}_{6.95}$, *Phys. Rev. B* 49 (1994) 12165–12169.
- [27] Y.J. Uemura, et al., Universal correlations between T_c and n_s/m^* (carrier density over effective mass) in high-Tc cuprate superconductors, *Phys. Rev. Lett.* 62 (1989) 2317–2320.
- [28] C.J. van der Beek, M. Konczykowski, A. Abal'oshev, I. Abal'osheva, P. Gierlowski, S.J. Lewandowski, M.V. Indenbom, S. Barbanera, Strong pinning in high-temperature superconducting films, *Phys. Rev. B* 66 (2002) 024523–024532.
- [29] B. Maiorov, S.A. Baily, H. Zhou, O. Ugurlu, J.A. Kennison, P.C. Dowden, T.G. Holesinger, S.R. Folty, L. Civale, Synergistic combination of different types of defect to optimize pinning landscape using BaZrO_3 -doped $\text{YBa}_2\text{Cu}_3\text{O}_7$, *Nat. Mater.* 8 (2009) 398–404.
- [30] M.P. Maley, J.O. Willis, H. Lessure, M.E. McHenry, Dependence of flux-creep activation energy upon current density in grain-aligned $\text{YBa}_2\text{Cu}_3\text{O}_7$, *Phys. Rev. B* 42 (1990) 2639–2642.
- [31] J.G. Ossandon, J.R. Thompson, D.K. Christen, B.C. Sales, Y. Sun, K.W. Lay, Flux-creep studies of vortex pinning in an aligned $\text{YBa}_2\text{Cu}_3\text{O}_7$ -superconductor with oxygen deficiencies $\delta \leq 0.2$, *Phys. Rev. B* 46 (1992) 3050–3058.
- [32] J.R. Thompson, L. Krusin-Elbaum, L. Civale, G. Blatter, C. Field, Superfast vortex creep in $\text{YBa}_2\text{Cu}_3\text{O}_{7-d}$ crystals with columnar defects: evidence for variable-range vortex hopping, *Phys. Rev. Lett.* 78 (1997) 3181–3184.
- [33] L. Civale, Vortex pinning and creep in high-temperature superconductors with columnar defects, *Supercond. Sci. Technol.* 10 (1997) A11–A29.
- [34] S. Eley, M. Leroux, M.W. Rupich, D.J. Miller, H. Sheng, P.M. Niraula, A. Kayani, U. Welp, W.-K. Kwok, L. Civale, Decoupling and tuning competing effects of different types of defects on flux creep in irradiated $\text{YBa}_2\text{Cu}_3\text{O}_{7-d}$ coated conductors, *Supercond. Sci. Technol.* 30 (2017) 015010.
- [35] N. Haberkorn, J. Guimpel, S. Suárez, H. Troiani, P. Granell, F. Golmar, Jae-hun Lee, S.-H. Moon, Hunju Lee, Strong influence of the oxygen stoichiometry on the vortex bundle size and critical current densities J_c of $\text{GdBa}_2\text{Cu}_3\text{O}_x$ coated conductors grown by co-evaporation, *Supercond. Sci. Technol.* 30 (2017) 095009.
- [36] T.R. Chien, W.R. Datars, B.W. Veal, A.P. Paulikas, P. Kostic, Chun Gu, Y. Jiang, Dimensional crossover and oxygen deficiency in $\text{YBa}_2\text{Cu}_3\text{O}_x$ single crystals, *Phys. C* 229 (1994) 273–279.